Optimization of FRM FIR Digital Filters Over CSD and CDBNS Multiplier Coefficient Spaces Employing a Novel Genetic Algorithm

Patrick Mercier, Sai Mohan Kilambi, and Behrouz Nowrouzian
Department of Electrical and Computer Engineering, University of Alberta, Edmonton, Alberta T6G-2V4, Canada
Email: {pmercier, skilambi, nowr}@ece.ualberta.ca

***Abstract*— It is well known that frequency response masking (FRM) FIR digital filters can be designed to exhibit very sharp-transition bands at the cost of slightly larger filter lengths as compared to the conventional FIR digital filters. The FRM FIR digital filters permit efficient hardware implementations due to an inherently large number of zero-valued multiplier coefficients in their transfer functions. The hardware complexity of these FIR digital filters can be further reduced by employing computationally efficient number systems for the representation of the constituent non-zero-valued multiplier coefficients. This paper presents a novel genetic algorithm for the design and discrete optimization of FRM FIR digital filters over the conventional canonical signed-digit (CSD) as well as the emerging double base number system (DBNS) multiplier coefficient spaces. This genetic algorithm is based on a pair of indexed look-up tables (LUTs) of permissible CSD/DBNS numbers whose indices form a *closed set* under the genetic algorithm operations of crossover and mutation. The CSD/DBNS values themselves permit pre-specified wordlengths and pre-specified number of non-zero bits. The salient feature of the proposed genetic algorithm is that it automatically leads to legitimate CSD/DBNS multiplier coefficients without any recourse to gene repair during optimization. The main features of the proposed genetic algorithm are demonstrated through its application to the design of a pair of lowpass and bandpass FRM FIR digital filters.**

***Index Terms*— Frequency Response Masking Approach, Digital Filters, Genetic Algorithms, Optimization, Canonical Signed Digit, Double Base Number System.**

I. INTRODUCTION

A vast body of literature exists for the design of computationally efficient FIR digital filters [1]–[3] and their corresponding hardware implementations [4], [5]. In many practical applications, such as audio signal processing, FIR digital filters with sharp transition bands are required [6], [7]. Since the length of a FIR digital filter is inversely proportional to its transition bandwidth [2], [8], FIR digital filters with sharp transition bands lead to high computational complexity. Consequently, the resulting FIR digital filters occupy large chip areas and consume high amounts of power in their VLSI hardware implementations. In general, the multiplication operation is the most cost-intensive part in the VLSI hardware implementation. Therefore, there is every incentive to reduce the number of multiplication operations in the FIR digital filter realization.

The frequency response masking (FRM) FIR digital filter design technique employs lower order digital subfilters with gradual transition bands in such a manner as to realize very sharp transition bands in the overall FIR digital filter. The resulting FRM FIR digital filters turn out to have an inherently large number of zero-valued multiplier coefficients, leading to a substantial reduction in the computational complexity of the resulting FIR digital filter [3]. The constituent digital subfilters are designed by using popular FIR digital filter design techniques such as the Parks-McClellan approach [1]. A further reduction in the corresponding hardware complexity of the FRM digital filters can be achieved by constraining the multiplier coefficients values to conform to computationally-efficient number systems such as the signed power-of-two (SPT) system [9]. This number system permits the representation of the multiplier coefficients having only a few non-zero bits within the coefficient wordlength, permitting the decomposition of the multiplication operation into a finite series of shift and add operations.

FIR digital filters incorporating SPT multiplier coefficient representation are commonly referred to as "multiplierless" digital filters [9]. However, since the SPT representation of a given number is non-unique, it gives rise to redundancy in the multiplier coefficient representation. This redundancy can adversely affect the corresponding computational complexity due to repetitive recourse to compare operations.

The canonical signed-digit (CSD) and canonical DBNS (CDBNS) form a pair of practical special cases of the SPT number system which circumvent the above redundancy problem by limiting the number of non-zero bits in the number representation. If used in combination with subexpression sharing and elimination, the CSD/CDBNS multiplier coefficient representations can lead to substantial reduction in the cost of the VLSI hardware implementation of the FIR digital filters [5], [10].

In the case of CSD number system, no two (or more) non-zero bits can appear consecutively in the representation of the multiplier coefficients, reducing the maximum number of non-zero bits by a factor of two in terms of

This paper is based on "Design of FRM Digital Filters Over the CSD Multiplier Coefficient Space Employing Genetic Algorithms," by Patrick M. Mercier and Behrouz Nowrouzian, Proceedings of the 2006 IEEE International Conference on Acoustics, Speech and Signal Processing, Toulouse, France, May 2006.

shift and add operations [11]. The DBNS number systems, on the other hand, employ two orthogonal bases for a sparse two-dimensional multiplier coefficient representation [12].

One can distinguish between two different techniques for the optimization of FIR digital filters, namely, gradient-based and discrete optimization approaches. During the past few decades, a number of practical techniques have been developed for the gradient-based optimization of FIR digital filters. In [13], an integer programming technique was developed for the corresponding optimization over the SPT multiplier coefficient space. This approach is not suitable for the optimization of FRM FIR digital filters, mainly due to the fact that it optimizes the constituent digital subfilters separately, giving rise to sub-optimality. An optimization technique based on Remez Exchange algorithm may provide a speed advantage over the linear programming approach. However, it too suffers from a similar sub-optimality problem [14]. In [15], an alternative approach based on the unconstrained weighted least-squares criterion was developed for the simultaneous optimizations of the digital subfilters constituent in the FRM digital filter proper. Non-convex optimization approaches such as semi-definite programming and second-order cone programming have also been applied to the optimization of FRM digital filters [16], [17]. However, these techniques involve a large number of constraints that adversely effect the computational efficiency of the optimization.

Genetic algorithms (GAs) have emerged as promising candidates for the design and discrete optimization of FIR digital filters, particularly due to the fact that they are capable of automatically finding near-optimum solutions while keeping the computational complexity of the algorithm at moderate levels. They allow a robust search of the solution space through a parallel search in all directions without recourse to gradient information [18].

In this paper, a novel GA is developed for the design and optimization of FRM FIR digital filters over the CSD [19] and the CDBNS [20] multiplier coefficient spaces.

This paper is organized as follows: Section II presents an overview of FRM FIR digital filter design approach. Section III is concerned with a brief discussion of the CSD and CDBNS number systems. section IV gives a general overview of GAs. Section V presents a GA for the optimization of finite-precision FRM FIR digital filters. Section VI illustrates the proposed GA optimization through its application to the design of a lowpass and a bandpass FRM FIR digital filter over the CSD and CDBNS multiplier coefficient spaces. Finally, Section VII summarizes the main conclusions of the paper.

II. Overview of FRM FIR Digital Filter Design Approach

Let $H(z)$ represent the transfer function of a desired FRM FIR lowpass digital filter. Furthermore, let $H\left(e^{j\omega}\right)$ represent the frequency response associated with $H(z)$, where z (ω, respectively) represents the discrete-time complex (real, respectively) frequency-variable. In addition, let ω_p and ω_s represent, respectively, the pass-band edge and the stop-band edge frequencies associated with the magnitude frequency-response $\left|H\left(e^{j\omega}\right)\right|$, with $\Delta = (\omega_s - \omega_p)$ representing the corresponding transition bandwidth[1]. Finally, let $H_a(z)$ represent the transfer function of a linear phase low-pass FIR bandedge-shaping digital subfilter with a passband edge frequency of θ, and a stopband edge frequency of ϕ, and let $H_a\left(e^{j\omega}\right)$ represent its corresponding frequency response as shown in Fig. 1. In this way, if $H_b(z)$ represents a transfer function complimentary to $H_a(z)$, then [3], [21]

$$H_b(z) = z^{-(N-1)/2} - H_a(z). \tag{1}$$

The magnitude frequency response of the complementary digital filter $H_b(z)$ is shown in Fig. 2.

The desired FRM FIR digital filter transfer function $H(z)$ can be realized in terms of $H_a(z)$ and $H_b(z)$ in accordance with

$$H(z) = H_a\left(z^M\right)H_{ma}(z) + H_b\left(z^M\right)H_{mb}(z), \tag{2}$$

where $H_a\left(z^M\right)$ and $H_b\left(z^M\right)$ are obtained from $H_a(z)$ and $H_b(z)$ by interpolation, i.e. by replacing each unit-delay by M-unit delays as illustrated in Fig. 3, and where $H_{ma}(z)$ and $H_{mb}(z)$ represent masking digital subfilters (c.f. Figs. 4 and 6) suppressing the unwanted image bands in $H_a\left(z^M\right)$ and $H_b\left(z^M\right)$. The transition bandwidth of the resulting FIR digital filter is also scaled by the interpolation factor M, resulting in a narrow-transition bandwidth of Δ/M. The overall lowpass FRM FIR digital filter structure can be realized as shown in Fig 8.

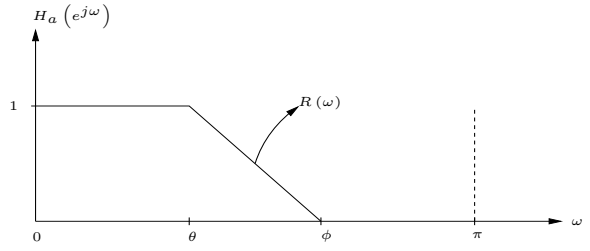

Figure 1. Magnitude Frequency Response of the Bandedge-Shaping Digital Subfilter $H_a(z)$ [3]

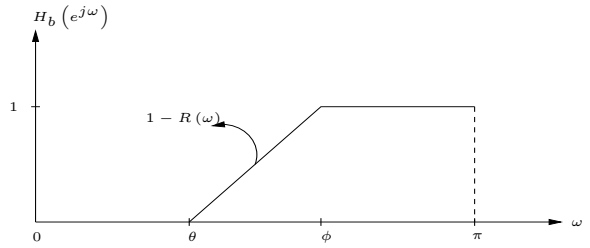

Figure 2. Magnitude Frequency Response of the Complementary Bandedge-Shaping Digital Subfilter $H_b(z)$ [3]

[1]Throughout this paper, it is tacitly assumed that the real frequency-variable ω as well as all the other angular frequencies, e.g. ω_p and ω_s, have been normalized to the Nyquist rate.

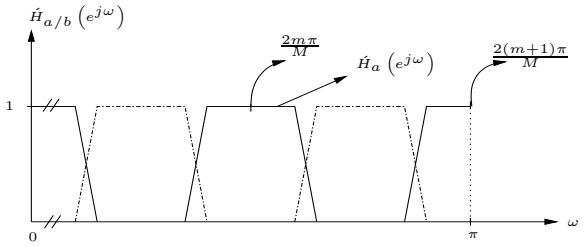

Figure 3. Magnitude Frequency Responses of the M-Interpolated Complementary Digital Subfilters $H_a\left(zM\right)$ and $H_b\left(zM\right)$ [3]

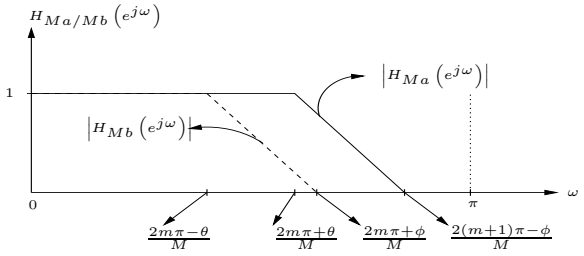

Figure 4. Magnitude Frequency Responses of the Masking Digital Subfilters $H_{Ma}\left(z\right)$ and $H_{Mb}\left(z\right)$ [3]

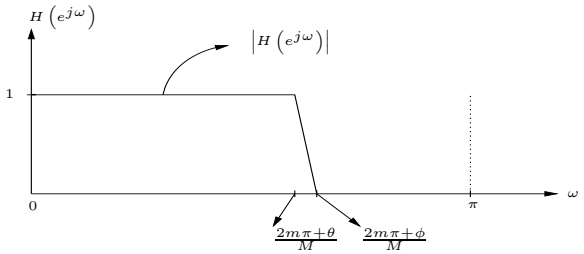

Figure 5. Magnitude Frequency Response of the Overall FRM FIR Digital Filter $H\left(z\right)$ [3]

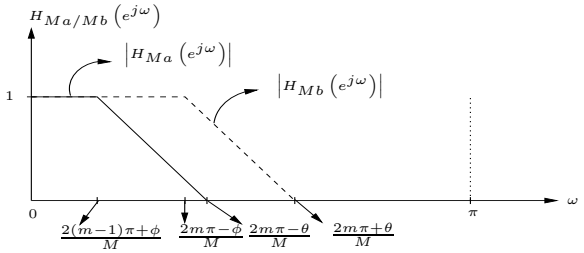

Figure 6. Magnitude Frequency Response of the Masking Digital Subfilters $H_{Ma}\left(z\right)$ and $H_{Mb}\left(z\right)$ [3]

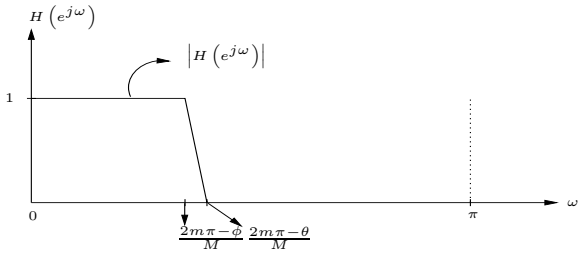

Figure 7. Magnitude Frequency Response of the Overall FRM FIR Digital Filter $H\left(z\right)$ [3]

III. CSD AND CDBNS MULTIPLIER COEFFICIENT REPRESENTATIONS

The optimization of an FRM FIR digital filter using the conventional techniques (e.g. Parks and McClellan approach [1]) results in a digital filter having infinite-precision multiplier coefficient values. In an actual hardware implementation of the digital filter, the infinite-precision multiplier coefficient values are replaced by their (fixed or floating-point) finite-precision counterparts. This paper is concerned with fixed-point multiplier coefficient representations employing CSD/DBNS number systems.

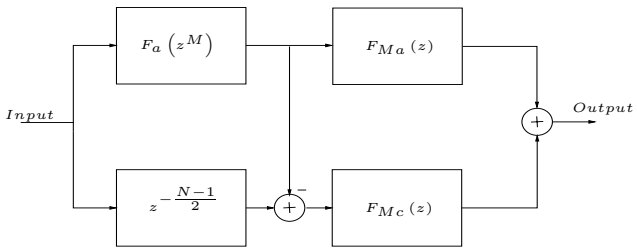

Figure 8. Realization of the Overall FRM FIR Digital Filter $H\left(z\right)$

A. CSD Representation

The CSD number system is a special case of the SPT system, but it leads to a unique representation of the given number. In the case of FRM FIR digital filters, the infinite-precision multiplier coefficient values x_j can be approximated to their fixed radix-point CSD counterparts $\hat{x_j}$ in accordance with

$$\hat{x_j} = \sum_{i=1}^{W} D_{ji} \times 2^{R-i}, \tag{3}$$

where W represents a pre-specified word-length, where w represents a pre-specified maximum number of non-zero bits, and where the integer R represents a radix-point in the range $0 < R < W$. Due to the following constraints

$$\begin{aligned} D_{ji} &\in \{1, -1, 0\} \\ D_{ji} \times D_{ji+1} &= 0 \\ \sum_{i=1}^{W} |D_{ji}| &\leq w \end{aligned} \tag{4}$$

in the CSD number system, the finite-precision multiplier coefficient values $\hat{x_j}$ may have very sparse representations, lending themselves to shift and add hardware implementations.

B. CDBNS Representation

In the case of the DBNS number system, the infinite-precision multiplier coefficient values x_j can be approximated to their fixed-point DBNS counterparts $\hat{x_j}$ in accordance with

$$\hat{x_j} = \sum_{k,\ l} d_{k,l} 2^k 3^l, \tag{5}$$

where $d_{k\ l} \in \{0,\ 1\}$, and where k and l are non-negative and independent integers [12]. In this way, when l is zero, the DBNS representation reduces to the binary representation. In general, a given number can have many

DBNS representations, but not all of the representations are efficient in terms of the total number of non-zero bits. Thus, the objective is to find a DBNS representation that has the least number of non-zero bits. The resulting representation is referred to as the canonical DBNS (CDBNS) representation. By using the greedy algorithm in [12], one may or may not be able to find the CDBNS representation for a given number. However, this algorithm will find a representation that is close to the CDBNS system. This leads to a near-canonic DBNS (NCDBNS) representation [12]. In this paper, the CDBNS numbers are assumed to have only one non-zero bit, bypassing the need for the aforementioned greedy algorithm altogether.

A direct approximation of multiplier coefficient values to their (finite-precision) CSD/DBNS counterparts leads to a FRM FIR digital filter that may no longer satisfy the given design specifications. However, the resulting FIR digital filter can be used as a seed digital filter in the GA to obtain a corresponding finite-precision FRM FIR digital filter which meets the desired design specifications.

IV. Genetic Algorithms

GAs are optimization techniques that are based on the natural selection and reproduction processes [22]. In general, GAs proceed in the following step-by-step manner [18]:

- *Initialization*: A seed chromosome is formed by concatenating the design variables converted into bit-strings. Subsequently, an initial population pool is generated by randomly complementing bits in the seed chromosome.
- *Evaluation*: Each chromosome in the population pool is evaluated against a fitness function and subsequently ranked.
- *Main optimization cycle*:
  1) *Generation of a Mating Pool*: A mating pool is generated by selecting the best-ranking chromosomes for reproduction. In addition, a few low-fitness chromosomes are also included in the mating pool to promote diversity.
  2) *Reproduction*: The next-generation population pool is generated by mating parent-pair chromosomes in the mating pool using genetic operations of crossover and mutation. The crossover operation causes the reproduction of new candidate chromosomes from existing ones. Mutation, on the other hand, is generally a background operation searching for other possible candidate chromosomes.
  3) Each offspring chromosome is evaluated against the fitness function and ranked. The resulting next-generation population pool usually consists of the best performing offspring chromosomes.

The above main optimization cycle is repeated until an acceptable solution is found.

The main differences [18], [22] between GAs and the conventional optimization techniques are:

- GAs do not require any gradient information to perform the optimization.
- GAs manipulate the design variables at the bit level rather than a direct manipulation of the variables themselves.
- GAs can perform a parallel search using a population of potential candidate chromosomes (derived by perturbing bits in a seed chromosome), making them very effective in finding optimum solutions to complex, multi-modal optimization problems.

Due to their inherent parallel search nature, GAs allow evaluation of many local optima, and can potentially find the global optimum. The parallel search capabilities are made possible by crossover and mutation operations.

V. The Proposed GA Optimization of FRM FIR Digital Filters

In the conventional optimization of FIR digital filters using GAs, the constituent multiplier coefficient values are replaced by their binary representations, and the resulting representations are concatenated to form a seed chromosome. The remaining members of the population pool are generated by complementing randomly selected bits in the seed chromosome. However, in the cases of CSD/CDBNS multiplier coefficient representations, complementing the selected bits in the seed chromosome may result in a chromosome which may no longer conform to the CSD/CDBNS number system[2]. In this paper, this problem is avoided altogether by generating a pair of indexed look-up tables (LUTs) of permissible CSD and CDBNS multiplier coefficient values in such a manner that the respective set of indices are closed under any GA operation (including the operation of complementing bits). In this way, the seed chromosome is formed by concatenating the binary representation of the CSD/CDBNS multiplier coefficient value indices (as opposed to the multiplier coefficient values themselves). Consequently, the seed chromosome will always result in chromosomes which conform to the original CSD/DBNS number systems.

The proposed GA for the optimization of FRM FIR digital filters over the CSD/CDBNS multiplier coefficient spaces is presented in the following.

A. Construction of CSD/CDBNS seed FRM FIR Digital Filter

The GA optimization of the FRM FIR digital filter $H(z)$ is conducted in terms of the multiplier coefficient values of the digital subfilters $H_a(z)$, $H_{ma}(z)$ and $H_{mb}(z)$. As before, the resulting CSD/CDBNS multiplier coefficient values are constrained to have a maximum of w non-zero bits within their wordlengths of W bits.

The initial CSD/CDBNS seed FRM FIR digital filter is obtained by approximating the multiplier coefficient values of a corresponding infinite-precision FRM FIR

[2]The same problem arises under the operations of crossover and mutation in the course of optimization by the underlying GA.

digital filter to their CSD/DBNS counterparts by using the above LUTs, where the infinite-precision multiplier coefficients themselves are generated by applying a conventional optimization technique (e.g. the Parks-Mclellan approach) to the digital subfilters $H_a(z)$, $H_{ma}(z)$ and $H_{mb}(z)$.

The generation of the proposed CSD and CDBNS LUTs is discussed next.

1) Generation of the CSD LUT: The CSD LUT is a two-column table consisting of CSD multiplier coefficient values and their corresponding ordered indices. Let the infinite-precision multiplier coefficient values lie in the range $\{-c_p,\ +c_p\}$. Moreover, let $W = W_I + W_F$, where W_I represents the wordlength of the integer part, and where W_F represents the wordlength of the fractional part of the CSD multiplier coefficient values. Then, W_I must be chosen such that the integer part of c_p can be represented in CSD. W_F, on the other hand, must be chosen based on the precision requirements of the FRM FIR digital filter application. For a fixed value of the wordlength W, a LUT of size L consisting of CSD numbers with a maximum of w non-zero bits is generated exhaustively. The LUT is subsequently trimmed to a size of 2^B, where B is the largest integer such that $2^B < L$. Then, the CSD numbers are assigned indices ranging from 1 to 2^B. It should be noted that the LUT size L may have to be increased so that after trimming, the CSD LUT would still be capable to representing the integer part of c_p in W_I bits.

Having constructed the above indexed CSD LUT, the infinite-precision multiplier coefficient values are approximated to their nearest CSD counterparts in the LUT. Then, the indices of the CSD multiplier coefficient values are converted to their B-bit binary strings and concatenated to form the desired seed CSD FRM FIR digital filter chromosome.

2) Generation of the CDBNS LUT: The CDBNS LUT is generated in much the same way as the CSD LUT, except that the CDBNS LUT consists of five columns, including the base 2 exponent, the base 3 exponent, the decimal equivalent of the CDBNS multiplier coefficient value, and the sign bit, in addition to the index column. The permissible CDBNS multiplier coefficient values are generated to lie in the range $\{-2^n3^m,\ 2^n3^m\}$, where the integer exponents n and m are chosen such that $2^n3^m > c_p$. The length of the resulting CDBNS LUT is $(2n+1)\times m$, which is trimmed to a size of 2^B (again, in order to form a closed set of indices under the GA operations).

In the same way as before, the infinite-precision multiplier coefficient values are approximated to their nearest CDBNS counterparts in the LUT, and the indices of the resulting CDBNS values are converted to B-bit strings and concatenated to form the desired seed chromosome.

B. Generation of the Initial Population Pool

By manipulating the resulting seed FRM FIR digital filter chromosome, a population pool of N chromosomes is generated. This manipulation involves the scanning of the seed chromosome B bits (i.e. one index) at a time, and by complementing the b^{th} bit (with $1 \le b \le B$) randomly in accordance with the probabilistic relationship $p_F \times 0.5^{B+1-b}$, where p_F is a fixed probability factor.

C. Fitness Evaluation

The fitness value of each of the N FRM FIR digital filter chromosomes is evaluated in accordance with

$$fitness = -20\log\left[\max\left\{\epsilon_p,\ \epsilon_s\right\}\right] + C, \tag{6}$$

where

$$\epsilon_p = \underbrace{max}_{\omega\in\Omega_p}\left[W_p\left|H\left(e^{j\omega}\right)-1\right|\right], \tag{7}$$

with Ω_p representing the passband frequency region(s), and where

$$\epsilon_S = \underbrace{max}_{\omega\in\Omega_s}\left[W_s\left|H\left(e^{j\omega}\right)\right|\right], \tag{8}$$

with Ω_s representing the stopband frequency region(s). Here, W_p and W_s are passband and stopband weighting factors, and C is a constant chosen so as to render the $fitness$ value in Eqn. 6 non-negative. In this way, the chromosomes in the population pool are ranked and sorted based on their fitness values. In the event that the resulting population pool does not contain a chromosome that satisfies the given design magnitude response specifications, the algorithm proceeds to generate the next-generation population pool. Otherwise, the algorithm terminates with the highest ranked chromosome declared as optimum.

D. Generation of Mating Pool

Having ranked the chromosomes based on their fitness values, a mating pool of size $N_{mating} < N$ is constructed by selecting chromosomes from the population pool using the relationship

$$p(x) = t^{1-x}Z^x, \tag{9}$$

where

$$t = \left(\frac{Z^N}{0.001}\right)^{1/(N-1)}, \tag{10}$$

where Z represents the probability of selecting a chromosome with a higher fitness value, and where x represents the fitness rank of the particular chromosome. It should be pointed out that Eqn. 9 is biased to select chromosomes with higher fitness values. In order to improve diversity, some non-elite chromosomes (i.e. chromosomes with low fitness values) are also incorporated in the mating pool.

E. Parent Selection

Parent chromosomes are selected from the mating pool by using the conventional roulette wheel selection method or correlative roulette wheel selection [23], [24]. This paper is concerned with general roulette wheel parent selection. Let $Total_{fit}$ represent the sum of the fitness values of the chromosomes in the entire mating pool. Then, a random number is generated to lie between 0 and

$Total_{fit}$. Consequently, the parent candidate chromosome is identified as such a chromosome for which the sum of its fitness value and the fitness values of all the preceding chromosomes in the mating pool is greater than or equal to this random number. This method is repeated until $N_p = \frac{N}{2}$ pairs of parent chromosomes have been selected.

F. Formation of the Next-Generation Population Pool

The next-generation population pool of size N is formed as discussed next:

- *Crossover Operations*: The parent chromosome pairs formed in the parent selection step undergo a two-point crossover operation, reproducing two offspring chromosomes per parent chromosome pair. This results in N offspring chromosomes which become members of the next-generation population pool.
- *Mutation Operations*: The chromosomes in the resulting next-generation population pool undergo mutation operations in accordance with the probabilistic relationship $p_M \times 0.5^{B+1-b}$ to enhance diversity, where p_M represents the probability of mutation.

VI. Application Examples

This section is concerned with the application of the proposed GA to the design and optimization of a pair of FRM FIR digital filters, one exhibiting a lowpass and the other a bandpass magnitude frequency response.

A. Lowpass FRM FIR Digital Filter Design Examples

Consider the design of a benchmark [3] lowpass FRM FIR digital filter satisfying the following magnitude response design specifications

Passband region	$0 \leq w \leq 0.6\pi$
Maximum passband ripple	± 0.1 dB
Stopband region	$0.61\pi \leq w \leq \pi$
Minimum stopband loss	40 dB

over the CSD/CDBNS multiplier coefficient spaces.

In order to obtain the corresponding infinite-precision lowpass FRM FIR digital filter, one has to select an appropriate value for the interpolation factor M such that the overall complexity of the FRM digital filter is at a minimum. This is achieved empirically, by evaluating the computational complexity of the FRM FIR digital filter for a range of values for M (e.g. for M from 2 to 14) as shown in Table I. From Table I, it is observed that an interpolation factor of $M = 6$ gives rise to the lowest FRM FIR digital filter total length, yielding digital subfilters $H_a(z)$, $H_{ma}(z)$ and $H_{mb}(z)$ of lengths 84, 24 and 42, respectively.

Having fixed the value of M at 6, the passband and stopband edge frequencies of the digital subfilters $H_a(z)$, $H_{ma}(z)$ and $H_{mb}(z)$ are determined by using the design equations given in [3]. Moreover, the passband ripple and stopband loss of these subfilters are set at 85% of the corresponding values given in the above design specifications (in order to account for any second order effects when using the design equations in [3]). In this way, the derived design specifications for the digital subfilters $H_a(z)$, $H_{ma}(z)$ and $H_{mb}(z)$ are obtained as shown in Table II.

TABLE I.
Filter Lengths for a Lowpass FRM FIR Digital Filter for Various Values of the Interpolation Factor M

M	H_a	H_{ma}	H_{mb}	Total Length
2	254	24	2	280
3	168	8	42	218
4	126	16	24	166
5	102	506	12	620
6	**84**	**24**	**42**	**150**
7	72	22	76	170
8	64	126	24	214
9	56	52	42	150
10	50	26	506	582
11	46	82	42	170
12	42	118	42	202
13	40	38	244	322
14	36	68	76	180

TABLE II.
Band-Edge Frequencies, Passband Ripples and Stopband Losses for Digital Subfilters $H_a(z)$, $H_b(z)$, $H_{ma}(z)$ and $H_{mb}(z)$

Subfilter	Passband Edge Frequency	Stopband Edge Frequency	Passband Ripple	Stopband Loss
H_a	0.34π	0.4π	0.085 dB	46 dB
H_b	0.4π	0.34π	0.085 dB	46 dB
H_{ma}	0.4π	0.61π	0.085 dB	46 dB
H_{mb}	0.6π	0.72π	0.085 dB	46 dB

Finally, by using the Parks McClellan approach, the subfilters $H_a(z)$, $H_{ma}(z)$ and $H_{mb}(z)$ can be designed to have magnitude frequency responses as shown in Figs. 9 to 10. Consequently, the magnitude frequency response

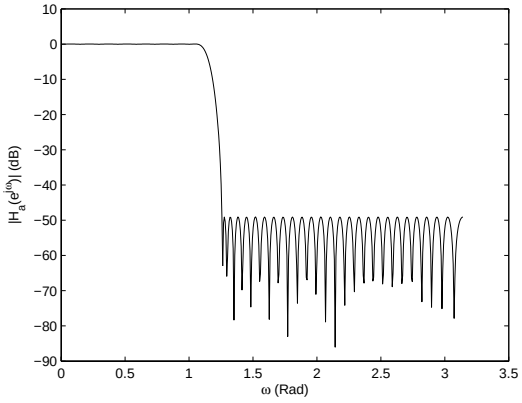

Figure 9. Magnitude Frequency Response of the Digital Subfilter $H_a(z)$

of the overall infinite-precision lowpass FRM FIR digital filter $H(z)$ is obtained as shown in Fig. 11.

1) CSD Lowpass FRM FIR Digital Filter GA Optimization: The design parameters for the genetic optimization of the CSD lowpass FRM FIR digital filter are as shown in Table III. Based on the above infinite-precision

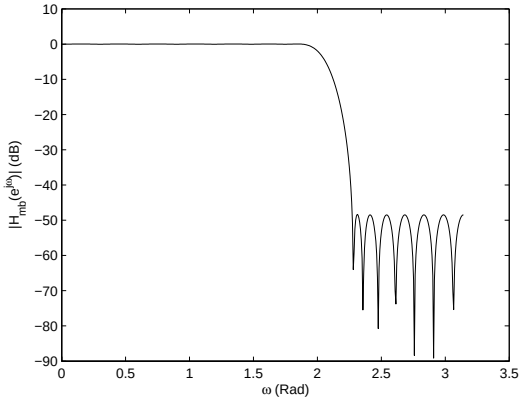

Figure 10. Magnitude Frequency Response of the Masking Digital Subfilter $H_{mb}(z)$

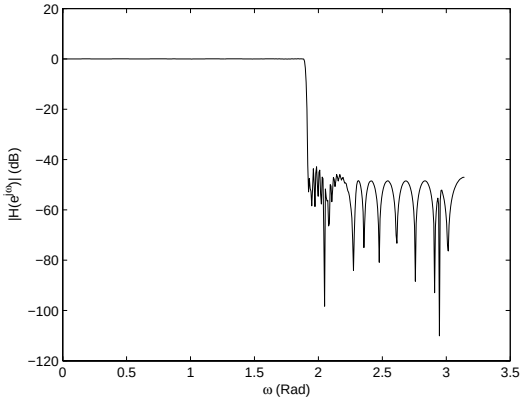

Figure 11. Magnitude Frequency Response of the Infinite-Precision Lowpass FRM FIR Digital Filter $H(z)$

lowpass FRM FIR digital filter, the corresponding CSD FRM seed digital filter is obtained to have a magnitude frequency response as shown in Fig. 12. It can be observed that the resulting seed digital filter violates the magnitude response specifications by almost 0.5 dB in the pass-band, and by almost 20 dB in the stop-band region

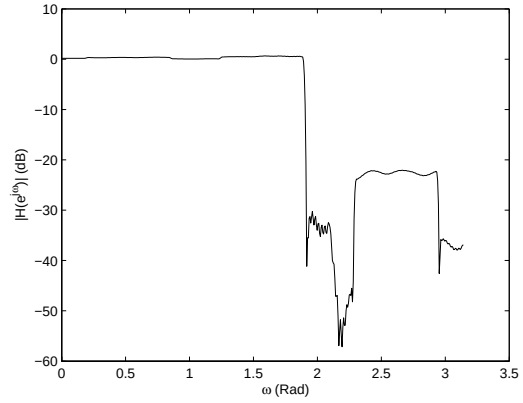

Figure 12. Magnitude Frequency Response of the Lowpass FRM FIR Digital Filter $H(z)$ after CSD Approximation

TABLE III.
DESIGN PARAMETERS FOR GA OPTIMIZATION OF CSD LOWPASS FRM FIR DIGITAL FILTER $H(z)$

Design Step	Design Parameters
A	$M = 6,\ N_a = 78,\ N_{ma} = 22,\ N_{mb} = 38$
$A1$	$w = 3,\ W_I = 3,\ W_F = 14\ , B = 12$
B	$p_F = 0.8,\ N = 500$
C	$C = 30$
D	$N_{mating} = 150,\ Z = 0.8$
E	$N_p = 235$
F	$p_M = 0.03$

(c.f. Table IV). By applying the proposed GA to the seed FRM digital filter, the GA evolves from one generation to the next with the average fitness of the population pool and the fitness of the top 50% individuals as shown in Fig. 13. It can be observed that the trend of the genetic optimization is towards individuals with increased fitness. After 1000 generations, the GA optimization converges to the optimal lowpass FRM FIR digital filter having a magnitude frequency response as shown in Fig. 14. It should be pointed out that the optimized CSD lowpass FRM FIR digital filter outperforms its infinite-precision

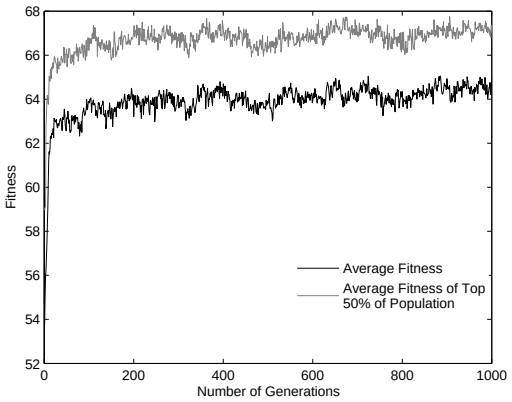

Figure 13. Fitness Evolution for CSD FRM FIR Lowpass Digital Filter $H(z)$

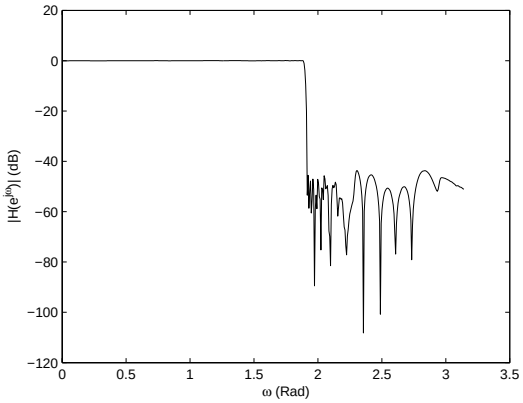

Figure 14. Magnitude Frequency Response of the CSD Lowpass FRM FIR Digital Filter $H(z)$ after GA Optimization

counterpart by 0.01 dB in the pass-band, and by almost 1 dB in the stop-band region (c.f. Table IV).

TABLE IV.
CSD LOWPASS FRM FIR DIGITAL FILTER MAGNITUDE RESPONSE CHARACTERISTICS BEFORE AND AFTER GA OPTIMIZATION

Multiplier Coefficient Representation	Passband Ripple	Stopband Loss
Infinite-Precision	0.075 dB	41 dB
CSD before GA Optimization	0.65 dB	22.05 dB
CSD after GA Optimization	0.05 dB	43.62 dB

2) CDBNS Lowpass FRM FIR Digital Filter GA Optimization: In the case of the GA optimization of the CDBNS lowpass FRM FIR digital filter, the design parameters are as shown in Table V. The corresponding

TABLE V.
DESIGN PARAMETERS FOR GA OPTIMIZATION OF THE CDBNS LOWPASS FRM FIR DIGITAL FILTER

Design Step	Design Parameters
A	$M = 6,\ N_a = 78,\ N_{ma} = 22,\ N_{mb} = 38$
$A2$	$n = 96,\ m = 69, B = 12\ bits$
B	$p_F = 0.8,\ N = 500$
C	$C = 30$
D	$N_{mating} = 150,\ Z = 0.8$
E	$N_p = 235$
F	$p_M = 0.03$

CDBNS FRM seed digital filter is obtained to have a magnitude frequency response as shown in Fig. 15, violating the magnitude response specifications by almost 0.046 dB in the passband, and by almost 3 dB in the stopband region (c.f. Table VI). By applying the proposed GA to the

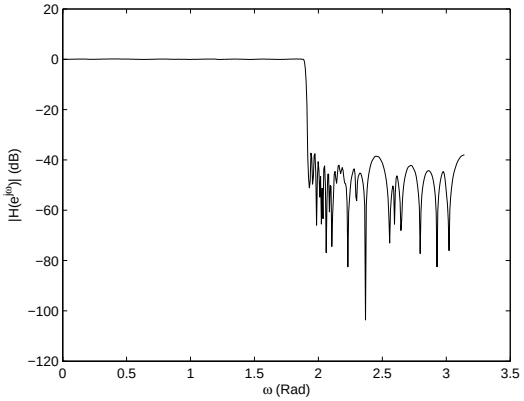

Figure 15. Magnitude Frequency Response of the Lowpass FRM FIR Digital Filter $H(z)$ after CDBNS Approximation

seed CDBNS FRM digital filter, the evolution of the GA from one generation to the next is as shown in Fig. 16. Fig. 17 shows the optimized CDBNS FRM FIR digital filter obtained after 1000 generations, outperforming its infinite-precision counterpart by almost 0.01 dB in the passband, and by almost 1 dB in the stopband region (c.f. Table VI).

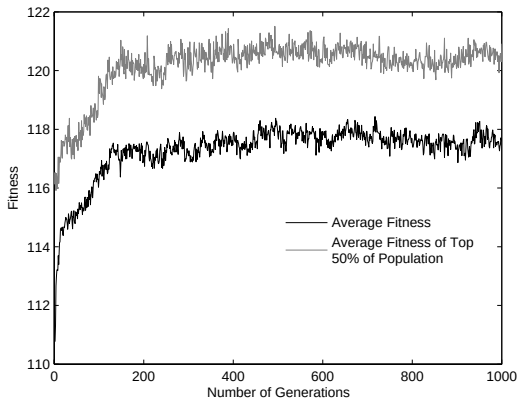

Figure 16. Fitness Evolution for the CDBNS Lowpass FRM FIR Digital Filter $H(z)$

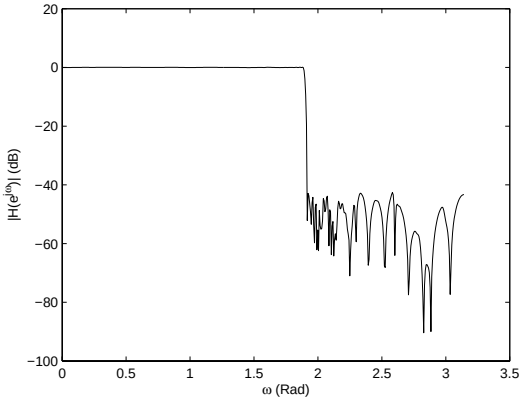

Figure 17. Magnitude Frequency Response of the CDBNS Lowpass FRM FIR Digital Filter $H_{LP}(z)$ after GA Optimization

TABLE VI.
CDBNS LOWPASS FRM FIR DIGITAL FILTER MAGNITUDE RESPONSE CHARACTERISTICS BEFORE AND AFTER GA OPTIMIZATION

Multiplier Coefficient Representation	Passband Ripple	Stopband Loss
Infinite-Precision	0.075 dB	41 dB
CDBNS before GA Optimization	0.146 dB	37.3 dB
CDBNS after GA Optimization	0.06 dB	42.62 dB

B. Design of bandpass FRM FIR digital filters

Bandpass FRM FIR digital filters can be designed in much the same as the corresponding lowpass FRM FIR digital filters except that $H_{ma}(z)$ and $H_{mb}(z)$ become bandpass masking digital filters. Let us consider the design of a FRM FIR bandpass digital filter satisfying the following magnitude response specifications over the

CSD/DBNS multiplier coefficient spaces.

Passband region	$0.15 \leq w/2\pi \leq 0.35$
Maximum pass-band ripple	± 0.1 dB
Lower stopband region	$0 \leq w/2\pi \leq 0.145$
Upper stopband region	$0.355 \leq w/2\pi \leq 0.5$
Minimum stopband loss	40 dB

From Table VII, the appropriate value for the interpolation factor M is found to be 8. This renders the

TABLE VII.
FILTER LENGTHS FOR BANDPASS FRM FIR DIGITAL FILTER FOR VARIOUS VALUES OF THE INTERPOLATION FACTOR M

M	H_a	H_{ma}	H_{mb}	Total Length
2	254	10	6	270
3	168	6	66	240
4	126	56	10	192
5	102	24	26	152
6	84	20	66	170
7	72	272	18	362
8	**64**	**32**	**56**	**152**
9	56	34	66	156
10	50	506	26	582
11	46	36	114	196
12	42	56	66	164
13	40	200	40	280
14	36	40	272	348

lengths of $H_a(z)$, $H_{ma}(z)$ and $H_{mb}(z)$ as 64, 32 and 56, respectively. Table VIII shows the derived design specifications for the digital subfilters $H_a(z)$, $H_{ma}(z)$ and $H_{mb}(z)$.

TABLE VIII.
BAND-EDGE FREQUENCIES, PASSBAND RIPPLES AND STOPBAND LOSSES FOR DIGITAL SUBFILTERS $H_a(z)$, $H_b(z)$, $H_{ma}(z)$ AND $H_{mb}(z)$

Subfilter	Passband Edge Frequencies	Stopband Edge Frequencies	Passband Ripple	Stopband Loss
H_a	0.32π	0.4π	0.085 dB	46 dB
H_b	0.4π	0.32π	0.085 dB	46 dB
H_{ma}	0.45π and 0.55π	0.29π and 0.71π	0.085 dB	46 dB
H_{mb}	0.3π and 0.7π	0.21π and 0.79π	0.085 dB	46 dB

By using the Parks McClellan approach, the digital subfilters $H_a(z)$, $H_{ma}(z)$ and $H_{mb}(z)$ can be designed to have magnitude frequency responses as shown in Figs. 18 to 19. Fig. 20 shows the magnitude frequency response of the overall infinite-precision bandpass FRM FIR digital filter $H(z)$.

1) CSD Bandpass FRM FIR Digital Filter GA Optimization: The design parameters for the genetic optimization of the CSD bandpass FRM FIR digital filter are shown in Table IX. Based on the above infinite-precision bandpass FRM FIR digital filter, the corresponding CSD FRM seed digital filter is obtained to have a magnitude frequency response as shown in Fig. 21. Consequently, the resulting seed digital filter violates the magnitude response specifications by almost 2 dB in the stopband region (c.f. Table X). The progress of the proposed GA from one generation to the next is as shown in Fig. 22. After 1000 generations, the GA optimization converges to the optimal bandpass FRM FIR digital filter having a magnitude frequency response as shown in Fig. 23.

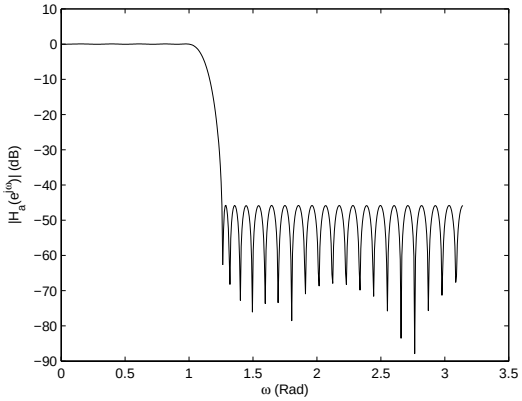

Figure 18. Magnitude Frequency Response of the Digital Subfilter $H_a(z)$

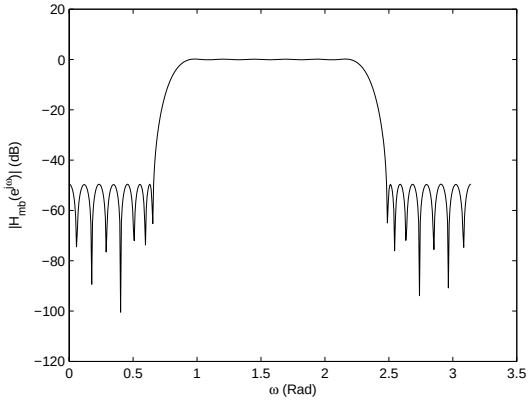

Figure 19. Magnitude Frequency Response of the Masking Digital Subfilter $H_{mb}(z)$

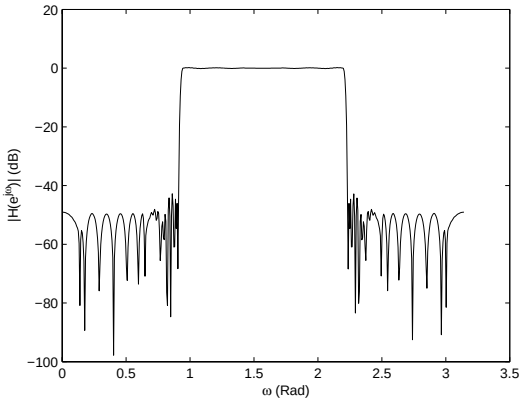

Figure 20. Magnitude Frequency Response of the Infinite-Precision Bandpass FRM FIR Digital Filter $H(z)$

2) CDBNS Bandpass FRM FIR Digital Filter GA Optimization: Table XI shows the design parameters for the GA optimization of the CDBNS bandpass FRM digital filter. The corresponding CDBNS FRM FIR seed digital filter is obtained to have a magnitude frequency response as shown in Fig. 24, violating the magnitude response

TABLE IX.
DESIGN PARAMETERS FOR THE GA OPTIMIZATION OF CSD BANDPASS FRM FIR DIGITAL FILTER $H(z)$

Design Step	Design Parameters
A	$M = 8,\ N_a = 64,\ N_{ma} = 32,\ N_{mb} = 56$
$A1$	$w = 3,\ W_I = 3,\ W_F = 14,\ B = 12$
B	$p_F = 0.8,\ N = 500$
C	$C = 30$
D	$N_{mating} = 150,\ Z = 0.8$
E	$N_p = 235$
F	$p_M = 0.03$

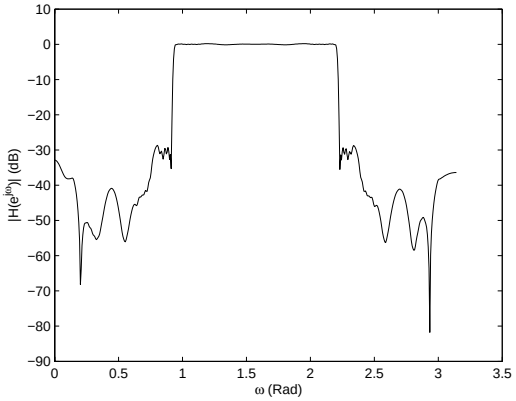

Figure 21. Magnitude Frequency Response of the Bandpass FRM FIR Digital Filter $H(z)$ after CSD Approximation

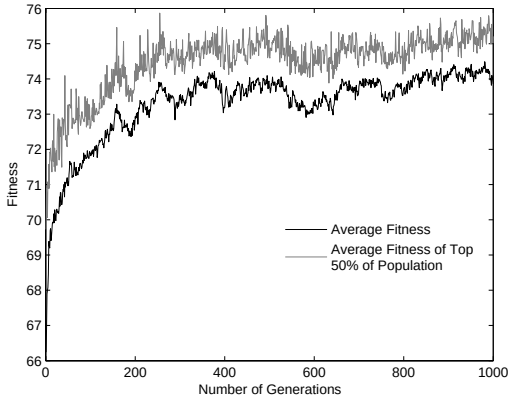

Figure 22. Fitness Evolution for the CSD FRM FIR Bandpass Digital Filter $H(z)$

specifications by almost 0.08 dB in the passband, and by almost 12 dB in the stopband region (c.f. Table XII). Fig. 25 shows the the progress of the proposed GA from one generation to the next. After 976 generations, the GA optimization converges to the optimal bandpass FRM FIR digital filter having a magnitude frequency response as shown in Fig. 26.

VII. CONCLUSION

This paper has presented a novel genetic algorithm (GA) for the design and discrete optimization of FRM FIR digital filters over the conventional canonical signed-digit (CSD) as well as the emerging canonical double

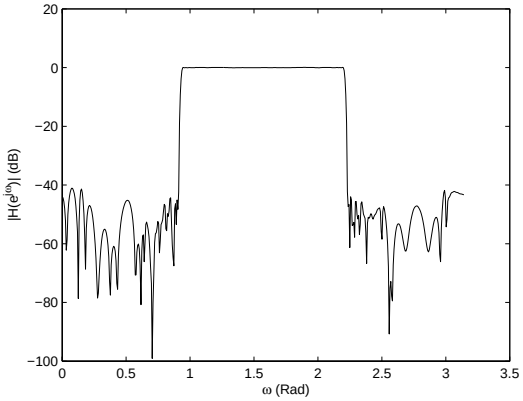

Figure 23. CSD Bandpass FRM FIR Digital Filter $H(z)$ after GA Optimization

TABLE X.
CSD BANDPASS FRM FIR DIGITAL FILTER MAGNITUDE RESPONSE CHARACTERISTICS BEFORE AND AFTER GA OPTIMIZATION

Multiplier Coefficient Values	Passband Ripple	Stopband Loss
Infinite-Precision	0.03 dB	50 dB
CSD before GA Optimization	0.06 dB	38.9 dB
CSD after GA Optimization	0.045 dB	46.3 dB

TABLE XI.
DESIGN PARAMETERS FOR GA OPTIMIZATION OF CDBNS BANDPASS FRM FIR DIGITAL FILTER

Design Step	Design Parameters
A	$M = 8,\ N_a = 64,\ N_{ma} = 32,\ N_{mb} = 56$
$A2$	$n = 96,\ m = 69, B = 12\ bits$
B	$p_F = 0.8,\ N = 500$
C	$\omega_p = 0.6\pi,\ \omega_s = 0.61\pi,\ k = \frac{1.15}{0.85},\ C = 30$
D	$N_{mating} = 150,\ Z = 0.8$
E	$N_p = 235$
F	$p_M = 0.03$

TABLE XII.
CDBNS BANDPASS FRM FIR DIGITAL FILTER MAGNITUDE FREQUENCY RESPONSE CHARACTERISTICS BEFORE AND AFTER GA OPTIMIZATION

Multiplier Coefficient Representation	Passband Ripple	Stopband Loss
Infinite-Precision	0.03 dB	50 dB
CDBNS before GA Optimization	0.18 dB	28.7 dB
CDBNS after GA Optimization	0.038 dB	47.2 dB

base number system (DBNS) multiplier coefficient spaces. This GA is based on a pair of indexed look-up tables (LUTs) of permissible CSD/DBNS numbers such that their indices form a *closed set* under the GA operations of crossover and mutation. These LUTs consist of CSD/DBNS numbers having pre-speified wordlengths and pre-specified number of non-zero bits. The salient feature of the proposed GA is that it automatically leads to legitimate multiplier coefficients without any recourse to gene repair. Although the proposed GA has been

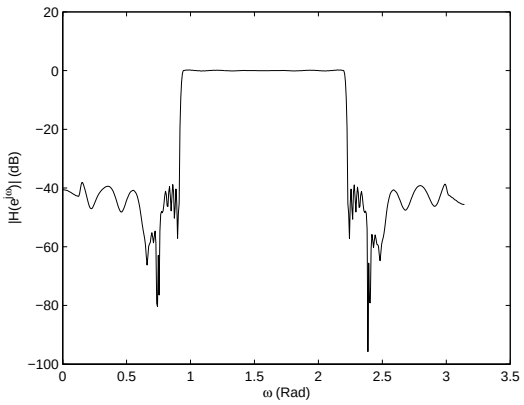

Figure 24. Magnitude Frequency Response of the Bandpass CDBNS FRM Digital Filter $H(z)$ before GA Optimization

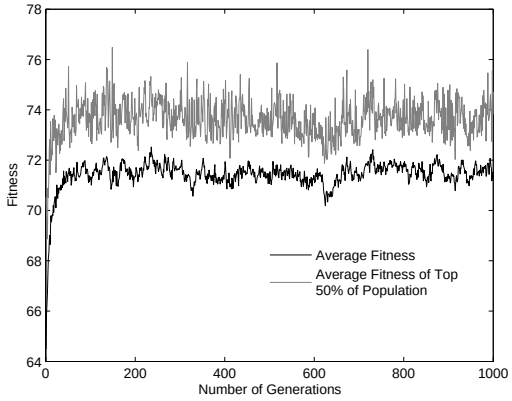

Figure 25. Fitness Evolution for CDBNS FRM FIR Bandpass Digital Filter

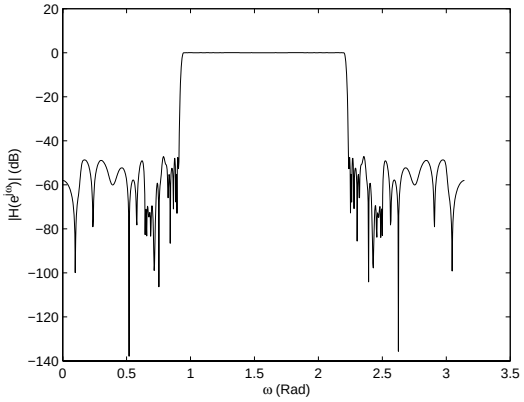

Figure 26. Magnitude Frequency Response of the Bandpass CDBNS FRM Digital Filter $H(z)$ after GA Optimization

developed in terms of a corresponding infinite-precision FRM FIR digital filter, it can be easily modified to begin with a finite-precision FRM FIR digital filter. In the latter case, the number of generations before obtaining an optimal FRM FIR digital filter may increase. The main features of the GA have been demonstrated through its application to the design of lowpass and bandpass FRM FIR digital filters. It has been shown that the resulting optimized CSD/CDBNS FRM FIR digital filters in some cases outperformed the corresponding infinite-precision FRM FIR digital filters.

ACKNOWLEDGMENT

This work was supported by a Natural Science and Engineering Research Council of Canada (NSERC) under the Discovery Grant $\#A6715$.

REFERENCES

[1] T. Parks and J. McClellan, “Cheyshev approximation for nonrecursive digital filters with linear phase.” *IEEE Trans. on Circuit Theory*, vol. CT-19, pp. 189–194, 1972.

[2] D. C. O. Hermann, L.R. Rabiner, “Practical design rules for optimum finite impulse response lowpass digital filters.” *Bell System Tech. J.*, vol. 52, pp. 769–799, 1981.

[3] Y. C. Lim, “Frequency-response masking approach for the synthesis of sharp linear phase digital filters,” *IEEE Transactions on Circuits and Systems*, vol. CAS-33, pp. 357–364, Apr 1986.

[4] H.-J. Kang and I.-C. Park, “Pairing and ordering to reduce hardware complexity in cascade form filter design [digital filters],” *ISCAS*, vol. 4, pp. 265–268, 25-28 May 2003.

[5] R. Hartley, “Subexpression sharing in filters using canonic signed digit multipliers,” *IEEE Trans. Circuits Syst. II*, vol. 43-10, pp. 677–688, Oct 1996.

[6] T. Sarmaki and A. Fam, “Subfilter approach for designing efficient fir filters.” *IEEE International Symposium on Circuits and Systems*, vol. 3, pp. 2903 – 2915, 7-9 June 1998.

[7] Y. C. Lim, “A digital filter bank for digital audio systems,” *IEEE Transactions on circuits and systems*, vol. 33-8, pp. 848 – 849, Aug. 1986.

[8] S. K. Mitra, *Digital Signal Processing - A Computer-Based Approach.* NY, NY: McGraw Hill, 2006.

[9] D. L. Yong Ching Lim, Rui Yang and J. Song, “Signed power-of-two term allocation scheme for the design of digital filters,” *IEEE Transactions on Circuits and Systems - Analog and Digital Signal Processing*, vol. II, pp. 577–584, May 1999.

[10] B. S. M. Potkonjak and A. Chandrakasan, “Multiple constant multiplication: Efficient and versatile framework and algorithms for exploring common subexpression elimination,” *IEEE Transactions on Computer-Aided Design*, vol. 15-2, pp. 151–165, 1996.

[11] F. A. A. fuller, B. Nowrouzian, “Optimization of fir digital filters over the canonical signed-digit coefficient space using genetic algorithms,” *Midwest Symposium on Circuits and Systems*, pp. 456–469, Aug. 1998.

[12] V. S. Dimitrov and G. A. Jullien, “Loading the bases: A new number representation with applications,” IEEE Circuits and Systems Magazine, Tech. Rep. 1540-7977, 2003.

[13] S. R. P. Yong Chin Lim and A. Constantinides, “Finite word length fir filter design using integer programming over a discrete coefficient space,” *IEEE Transactions on Acoustics, Speech and Signal Processing*, vol. ASSP-30, pp. 661–664, Aug. 1982.

[14] T. Sarmaki and Y. C. Lim, “Use of the remez algorithm for designing fir filters using the frequency response masking approach,” *IEEE conference on Circuits and Systems*, vol. III, pp. 449–455, 1999.

[15] Y. J. Yu and Y. C. Lim, “Frm based fir filter design - the wls approach,” *IEEE International Symposium on Circuits and Systems*, vol. III, pp. 221–224, May 2002.

[16] W.-S. Lu and T. Hinamoto, "Optimal design of frequency-response-masking filters using semidefinite programming," *IEEE Transactions on Circuits and Systems*, vol. 5, pp. 557–568, Apr. 2003.
[17] ——, "Optimal design of fir frequency-response-masking filters using second-order cone programming," *IEEE International Symposium on Circuits and Systems*, vol. 3, pp. 878–881, May 2003.
[18] D. Suckley, "Genetic algorithm in the design of fir filters," *IEEE Proceedings G.*, vol. 138, pp. 234–238, April 1991.
[19] P. Mercier and B. Nowrouzian, "Design of frm digital filters over the csd multiplier coefficient space employing genetic algorithms," *Proceedings of the 2006 IEEE International Conference on Acoustics, Speech and Signal Processing*, vol. 3, pp. 968–971, May 2006.
[20] ——, "A genetic algorithm for the design and optimization of frm digital filters over a canonical double base multiplier coefficient space." *Proceedings of 2006 IEEE ISCAS*, pp. 3289–3292, May 2006.
[21] Y. C. L. Rui Yang and S. R. Parker, "Design of sharp linear-phase fir bandstop filters using the frequency response-masking technique," *Circuits System Signal Processing*, vol. 17, pp. 1–27, 1998.
[22] D. E. Goldberg, *Genetic Algorithms in Search, Optimization, and Maching Learning*. Reading, MA: Addison-Wesley, 1989.
[23] S. Kilambi and B. Nowrouzian, "A novel genetic algorithm for optimization of frm digital filters over dbns multiplier coefficient space based on correlative roulette selection." *IEEE International Symposium on Signal Processing and Information Technology*, pp. 228–231, Aug 2006.
[24] ——, "A genetic algorithm employing correlative roulette selection for optimization of frm digital filters over csd multiplier coefficient space," *IEEE APCCAS*, vol. in press, Apr 2006.

Patrick Mercier received the B.Sc. degree in electrical and computer Engineering from the University of Alberta, Edmonton, Alberta, Canada, in 2006. He is currently pursuing the M.Sc. degree at the Massachusetts Institute of Technology (MIT) in Cambridge, MA, U.S.A.

His research interests include the design of energy efficient RF and digital circuits and systems for wireless communication applications. He was the recipient of a Julie Payette Natural Sciences and Engineering Research Council of Canada (NSERC) Postgraduate Research Scholarship in 2006.

Sai Mohan Kilambi received the B.Sc. degree in systems and computers engineering with high distinction from the Carleton University, Ottawa, Ontario, Canada, in 2004, and the M.Sc. degree in electrical and computer engineering from the University of Alberta, Edmonton, Alberta, Canada, in 2007.

Currently, he is working as a DSP ASIC/FPGA designer at Nortel Networks, Ottawa, Ontario, Canada.

Behrouz Nowrouzian received the B.Sc. degree in electrical engineering from Arya-Mehr (Sharif) University of Technology, Tehran, Iran, in 1975. He received the M.Sc., D.I.C., and Ph.D. degrees from the Imperial College of Science and Technology, University of London, London, U.K., in 1976, 1977, and 1983, respectively.

He was a member of Micronet, a network funded by Industry and the Federal Government of Canada under the Network of Centres of Excellence (NCE) program from 1991 to 2005.

Currently, he is a Professor at the Department of Electrical and Computer Engineering, University of Alberta, Edmonton, Alberta, Canada. His main research interests include VLSI digital signal processing, computer arithmetic and architecture, high-level synthesis, and application of optimization to circuits and systems.